

Long distance part of ε_K from lattice QCD

Ziyuan Bai*

Columbia University in the city of New York

E-mail: zb2174@columbia.com

We demonstrate the lattice QCD calculation of the long distance contribution to ε_K . Due to the singular, short-distance structure of ε_K , we must perform a short-distance subtraction and introduce a corresponding low-energy constant determined from perturbation theory, which we calculate at Next Leading Order (NLO). We perform the calculation on a $24^3 \times 64$ lattice with a pion mass of 329 MeV. This work is a complete calculation, which includes all connected and disconnected diagrams.

34th annual International Symposium on Lattice Field Theory

24-30 July 2016

University of Southampton, UK

*Speaker.

1. Introduction

The $K^0 - \bar{K}^0$ mixing parameter ϵ_K , with an experimental value of $2.228(11) \times 10^{-3}$, provides a measure of indirect CP violation in $K^0 - \bar{K}^0$ mixing. This amplitude is caused by $\Delta S = 2$ weak interaction and is second order in the Fermi constant G_F . Two types of diagrams which contribute to this process are shown in Fig. 1. The usual estimation from the standard Model of ϵ_K involves only the short distance contribution, calculated by first integrating out the W boson and top quark, resulting in a bi-local effective weak Hamiltonian. One then integrates out the charm quark and treats the bi-local weak Hamiltonian as a local operator multiplied by a Wilson coefficient determined in perturbation theory. We have seen a $3.6(2) \sigma$ tension between the experimental value if we use the exclusive V_{cb} while the tension goes away if use choose to use inclusive V_{cb} [2].

To understand the Standard Model contribution to ϵ_K , a calculation with the long distance part correctly controlled is needed. The previous estimation from Chiral Perturbation Theory is a few percent [4]. The calculation including the long distance part can be done using lattice QCD to calculate the bi-local part of the $K^0 - \bar{K}^0$ mixing matrix element and correcting the short distance divergence of the lattice calculation by performing a perturbative matching. In our first attempt [6], we have included the type 1&2 diagrams in our analysis and performed the perturbative matching to LO, which gave us a quite large systematic error because the NLO correction can be 50%. In this calculation, we have included all the diagrams and use a NLO perturbative matching with the effective Hamiltonian instead of matching to the box diagram in full theory.

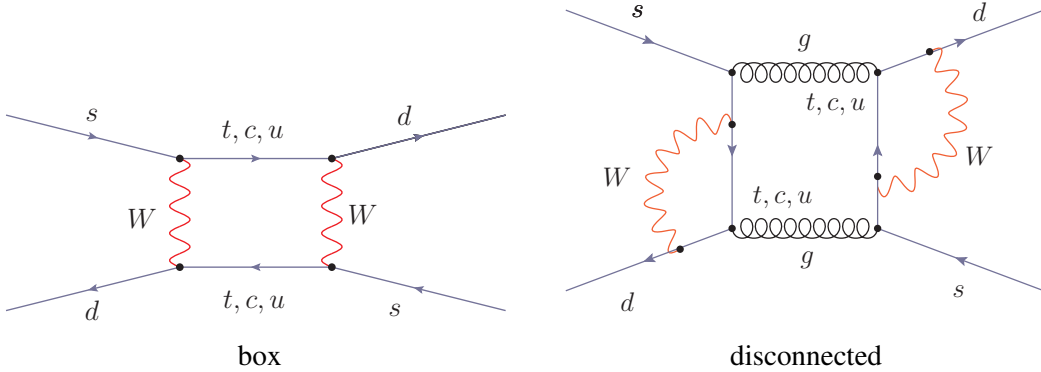


Figure 1: Two type of diagrams contribute to the $\Delta S = 2$ process.

2. Effective $\Delta S = 2$ Hamiltonian

The parameter ϵ_K can be calculated using Eq. 2.1, where $\phi_\epsilon = 43.52 \pm 0.005^\circ$, and ξ is the ratio of imaginary part of $K^0 \rightarrow \pi\pi$ matrix element A_0 to its real part. ΔM_K is the $K_L - K_S$ mass difference which has the experimental value $3.483(6) \times 10^{-12}$ MeV. We will have to calculate the imaginary part of the kaon mixing matrix element $M_{00} = \frac{\langle \bar{K}^0 | H_W^{\Delta S=2} | K^0 \rangle}{2m_K}$ from the Standard Model. The conventional method to calculate M_{00} involves first integrating out W boson and top quark, and then integrating out charm to get the weak Hamiltonian in Eq. 2.2. In writing out the effective Hamiltonian, we use a slightly different approach: we use the unitary condition of CKM matrix to

convert the sum over three up-type flavors in the internal quark lines into three pieces: $(u - c) \times (u - c)$, $(t - c) \times (t - c)$, and $(t - c) \times (u - c)$. This is different from subtracting the up quark in each piece which is commonly done. With our choice, we only have to consider the term that has $\lambda_u \lambda_t$ and involves the combination $(t - c) \times (u - c)$, because the other two terms are either purely a short-distance contribution, or do not receive an imaginary part from the CKM matrix.

$$\varepsilon_K = \exp i\phi_\varepsilon \sin \phi_\varepsilon \left(\frac{-\text{Im}M_{00}}{\Delta M_K} + \xi \right) \quad (2.1)$$

$$H_{\text{eff}}^{\Delta S=2} = \frac{G_F^2}{16\pi^2} M_W^2 [\lambda_u^2 \eta_1' S_0'(x_c) + \lambda_t^2 \eta_2' S_0'(x_t) + 2\lambda_u \lambda_t \eta_3' S_0'(x_c, x_t)] Z(\mu) Q_{LL} \quad (2.2)$$

To perform a long distance calculation, we do not integrate out the charm quark in $H_{\text{eff},ut}^{\Delta S=2}$, where to ut means the term contains a $\lambda_u \lambda_t$ factor. Instead, we calculate in the four flavor theory where we can expand the weak Hamiltonian as a sum over products of pairs of $\Delta S = 1$ operators, as shown in Eq. 2.3.

$$H_{\text{eff},ut}^{\Delta S=2} = \frac{G_F^2}{2} \lambda_u \lambda_t \left[\sum_{i=1}^2 \sum_{j=1}^6 C_i(\mu) C_j(\mu) [Q_i Q_j] + C_7(\mu) O_{LL} \right], \quad (2.3)$$

In Eq. 2.3, $Q_{1,2}$ are the current-current operators and $Q_{3,4,5,6}$ are the QCD penguin operators, whose definitions can be found in [3]. The structure of the product of operators $[Q_i Q_j]$ can be found in Eq.12.40 - 12.41 of [3], where the only difference is that we have a factor of $c - u$ propagator difference times a c propagator, instead of a $u - c$ times a u propagator. The operator $O_{LL} = (\bar{s}d)_{V-A}(\bar{s}d)_{V-A}$ is the local operator which changes the strangeness by 2. The product $[Q_i Q_j]$ will be logarithmically divergent when these two operators become close to each other because we do not have a GIM cancellation in both of the internal quark lines. This divergence will be absorbed by the Wilson coefficient of the operator Q_{LL} . In the lattice calculation, this quantity will also be ultra-violet divergent with the high energy cutoff determined by the inverse lattice spacing $1/a$. This divergence is unphysical and we have to remove it by subtracting the O_{LL} operator multiplied by a coefficient matched to the continuum. This matching will require a non-perturbative calculation on the lattice and a corresponding perturbative calculation in the continuum. This is done in an Regularization Independent (RI) intermediate scheme. To define our RI scheme, we write our RI operator in terms of both the \overline{MS} operator (Eq. 2.4) and the lattice operator (Eq. 2.5), we then impose the RI condition that these operators vanish when inserted in a Landau gauge-fixed Green's function evaluated at off-shell momenta with a scale $\mu_{RI} \gg \Lambda_{QCD}$. We can find both the coefficients $X^{i,j}$ and $Y^{i,j}$ in Eq. 2.4 and Eq. 2.5. This procedure is similar to what we have done in the $K \rightarrow \pi \nu \bar{\nu}$ calculation [7], but here we write our formula in a fashion in which we absorb some Wilson coefficients into X and Y .

$$[Q_i Q_j]^{RI}(\mu_{RI}) = Z_i^{lat \rightarrow RI}(\mu_{RI}, a) Z_j^{lat \rightarrow RI}(\mu_{RI}, a) \left\{ [Q_i Q_j]^{lat} - X^{i,j}(\mu_{RI}, a) O_{LL}^{lat} \right\}, \quad (2.4)$$

$$[Q_i Q_j]^{RI}(\mu_{RI}) = Z_i^{\overline{MS} \rightarrow RI}(\mu, \mu_{RI}) Z_j^{\overline{MS} \rightarrow RI}(\mu, \mu_{RI}) \left\{ [Q_i Q_j]^{\overline{MS}} - Y^{i,j}(\mu, \mu_{RI}) O_{LL}^{\overline{MS}} \right\}. \quad (2.5)$$

In Eq. 2.5, we will insert external momentum at scale μ_{RI} to evaluate the quantity $Y^{i,j}$. The conventional SM calculation of ε_K includes integrating out the charm quark, which is a similar calculation and is usually done at zero external momentum. Therefore, we define $\Delta Y^{i,j}(\mu, \mu_{RI})$ as the difference between $Y^{i,j}(\mu, \mu_{RI})$ evaluated at our μ_{RI} external momentum and the same quantity evaluated at zero external momentum. We can then write the total $\Delta S = 2$ weak Hamiltonian in a very clean way:

$$\begin{aligned}
H_{eff,ut}^{\Delta S=2} = & \sum_{i=1}^2 \sum_{j=1}^6 \left\{ C_i^{lat}(\mu) C_j^{lat}(\mu) \left([Q_i Q_j]^{lat} - X^{i,j}(\mu_{RI}) O_{LL}^{lat} \right) \right. \\
& + C_i^{\overline{MS}}(\mu) C_j^{\overline{MS}}(\mu) \left[Y_{\overline{MS}}^{i,j}(\mu, \mu_{RI}) - Y_{\overline{MS}}^{i,j}(\mu, 0) \right] Z^{lat \rightarrow \overline{MS}} O_{LL}^{lat} \\
& \left. + \left[C_i^{\overline{MS}}(\mu) C_j^{\overline{MS}}(\mu) Y_{\overline{MS}}^{i,j}(\mu, 0) + C_7^{\overline{MS}}(\mu) \right] Z^{lat \rightarrow \overline{MS}} O_{LL}^{lat} \right\}. \quad (2.6)
\end{aligned}$$

The first line of Eq. 2.6 involves the lattice operators and the coefficients $X^{i,j}$ determined from non-perturbative renormalization (NPR). We call this term the ‘‘contribution below μ_{RI} ’’, which includes the long distance part, and use $\text{Im} M_{00}^{ut,RI}(\mu_{RI})$ to denote its contribution to the kaon mixing matrix element. The second line involves coefficient $\Delta Y_{\overline{MS}}^{i,j}(\mu_{RI}) = Y_{\overline{MS}}^{i,j}(\mu, \mu_{RI}) - Y_{\overline{MS}}^{i,j}(\mu, 0)$ calculated from perturbation theory, and we call this term ‘‘perturbative RI to \overline{MS} correction’’, $\text{Im} M_{00}^{ut,RI \rightarrow \overline{MS}}(\mu_{RI})$. The last term is the result of conventional standard model calculation. We will label it the ‘‘conventional short distance result’’. The combination of the first two terms is our ‘‘long distance correction’’ to the SM calculation of ε_K . It should be independent of the RI scale μ_{RI} we introduced. The perturbative calculation of $\Delta Y_{\overline{MS}}^{i,j}(\mu_{RI})$ is illustrated in Fig 2. We note that this calculation is both infra-red and ultra-violet convergent at NLO, because of the non-zero charm quark mass and the subtraction between two logarithmically UV divergent diagrams. The NPR calculation of $X^{i,j}$ is the same as what we have done in [6].

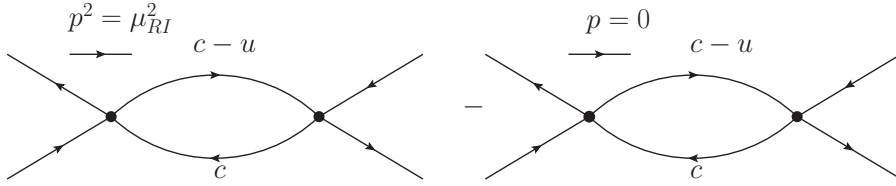


Figure 2: Illustration of the perturbative calculation of $\Delta Y_{\overline{MS}}^{i,j}(\mu_{RI})$

3. Lattice calculation and results

We have carried out this calculation on our $24^3 \times 64$ Iwasaki gauge ensemble with an inverse lattice spacing 1.78 GeV and a pion mass 338 MeV. The kaon mass is 591 MeV which is below the two pion energy. The charm quark is unphysical with a mass of 968 MeV. We use the method we introduced in the unphysical ΔM_K calculation [5], integrating over the position of the two weak Hamiltonians, and subtracting the contribution of all intermediate states lighter than the kaon, which in this case are the vacuum and the single pion state. We have contractions between two

current-current operators or between one current-current operator and one QCD penguin operator. We have 5 types of four point diagrams to compute on the lattice, where the type 5 diagram will only appear when we have a penguin operator. All the different contractions are shown in Fig 3. The type 1,2,3,4 diagrams are shown with two current-current operators and have $c \times (c - u)$ propagator combinations in the internal loop. For the diagram with one current-current operator and one penguin operator, we will have a $cc - uu$ difference for the propagators in the internal loop and $(c - u) \times (u + d + s + c)$ in the self loops of type 3&4 diagrams. The type 5 diagram shown has a vertex of $\bar{s}d\bar{s}s$ on the left, and we also have a similar diagram with a $\bar{s}d\bar{d}d$ vertex.

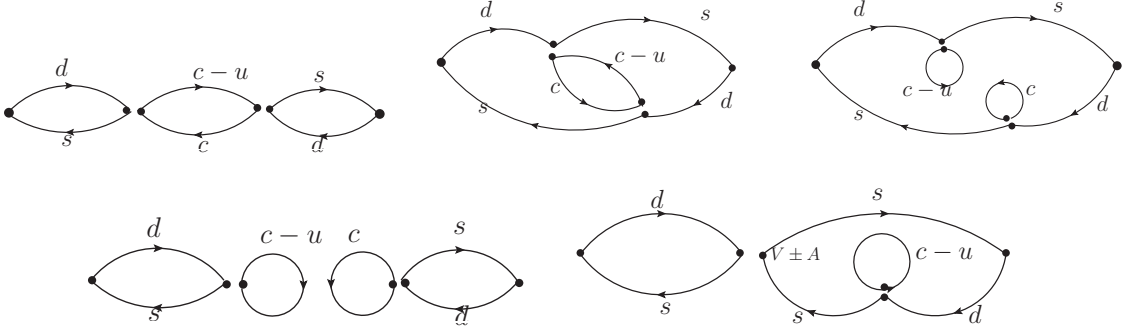


Figure 3: Five types of contractions appearing in this calculation. On the top: type 1,2,3 diagrams and on the bottom, type 4,5 diagrams, listed from left to right.

We have used Coulomb gauge fixed wall source for the two kaons, and we solve for a source at each time slice so we can perform a time translation for all the contractions we calculate. In the type 1&2 diagrams, we have used a point source at each time slice for one of the two weak vertices, while the other weak vertex is summed over the spacial volume. For the type 3&4 diagrams, the self-loop is computed with an all-to-all propagator whose high-mode part is obtained from a sum of 60 random, space-time volume sources, while the low mode part is constructed from 450 eigenvectors obtained from the Lanczos algorithm. In the type 5 diagrams, we use the same point source propagator as in the type 1&2 diagrams for the self-loop arising from the current-current operators, and the vertex of the penguin operators is summed over the spacial volume. In our first measurement, we had problems with our random number generator so we measured the type 3&4 diagrams again. In this analysis we used 75 configurations with a correct random number generator for type 3&4 diagrams and 150 configurations for type 1&2&5 diagrams which do not require random numbers.

Our lattice calculation of $\text{Im} M_{00}^{ut,RI}$, which corresponds to the contribution from those parts of H_W in the first line of Eq. 2.6, is shown in Table 1. We have listed the result from the different operator combinations and the Wilson coefficients have been included and the divergence has been removed by including the $X^{i,j}(\mu_{RI})$ terms. We can see that the current-current operators give the largest contributions because of their larger Wilson coefficients. We have shown the lattice Wilson coefficient for each operator in Table 2.

The sum over all terms in Table 1 is $\text{Im} M_{00}^{ut,RI} = -1.49(69)$, and its total contribution to ϵ_K is $|\epsilon_K^{ut,RI}| = 3.0(14) \times 10^{-4}$. To get our final correction to ϵ_K , we must include the second line of Eq. 2.6, which we call $\text{Im} M_{00}^{ut,RI \rightarrow \overline{MS}}$. This result is summarized in Table 3, and we

Q_1Q_1	Q_1Q_2	Q_1Q_3	Q_1Q_4	Q_1Q_5	Q_1Q_6
	Q_2Q_2	Q_2Q_3	Q_2Q_4	Q_2Q_5	Q_2Q_6
-0.4436(321)	0.2540(1364)	0.0696(112)	-0.0004(206)	-0.0228(173)	0.1701(1479)
	-1.6991(2232)	0.0284(201)	0.1405(419)	-0.0310(448)	0.2220(3850)

Table 1: Contribution to $\text{Im}M_{00}^{ld}$ by different operator combination, all 5 types of diagrams have been included. We have chosen $\mu_{RI} = 1.92$ GeV. From correlated fit with fitting range 8:16.

C_1	C_2	C_3	C_4	C_5	C_6
0.2373(1)	0.6885(1)	0.0113(6)	0.0213(7)	0.0085(6)	0.0256(6)

Table 2: Lattice Wilson coefficient, calculated using (γ_μ, γ_μ) intermediate scheme in the NPR step, and the \overline{MS} Wilson coefficient are obtained with $\mu = 2.15$ GeV.

have five different intermediate values for μ_{RI} to test the consistency of our result. In calculating $\text{Im}M_{00}^{ut,RI \rightarrow \overline{MS}}$, we have to specify the charm quark mass to be used in the perturbative calculation. Because this is a NLO calculation and our answer is accurate to order $\mathcal{O}(\alpha_s \ln \mu/M_W)$. The charm quark mass has a dependence on the scale $\mu_{\overline{MS}}$ or μ_{RI} , which is of order α_s , allowing us to ignore the scale dependence of charm quark mass and use a mass of 968 MeV, which is same as our lattice input converted to \overline{MS} at 2 GeV (We have used $Z_m^{lat \rightarrow \overline{MS}}(2 \text{ GeV}) = 1.498$ from [1]). The $\text{Im}M_{00}^{ut,RI \rightarrow \overline{MS}}$ contribution also involves the calculation of the kaon bag parameter B_K , which also has a scale dependence on $\mu_{\overline{MS}}$, and we have used the B_K evaluated at 2.15 GeV. We can see some dependence on μ_{RI} in Table 3. We found that the matching from the RI scheme to \overline{MS} is successful that the results in the last column, which is our long distance correction to ϵ_K , depend very little on the intermediate scale μ_{RI} (when the μ_{RI} is larger than 2 GeV). If we see a discrepancy between different μ_{RI} , then it might indicate we'll need a NNLO $\text{Im}M_{00}^{ut,RI \rightarrow \overline{MS}}$ to get a more consistent result. In such a NNLO matching, we must take the scale dependence of m_c and B_K into consideration.

μ_{RI}	$\text{Im}M_{00}^{ut,RI}$	$\text{Im}M_{00}^{ut,RI \rightarrow \overline{MS}}$	$\text{Im}M_{00}^{ut,ld corr}$	contribution to ϵ_K
1.54	-1.12(52)	0.352	-0.77(52)	$0.151(102) \times 10^{-3}$
1.92	-1.31(51)	0.476	-0.83(51)	$0.164(100) \times 10^{-3}$
2.11	-1.40(52)	0.537	-0.86(52)	$0.170(102) \times 10^{-3}$
2.31	-1.47(51)	0.599	-0.87(51)	$0.171(100) \times 10^{-3}$
2.56	-1.55(51)	0.674	-0.87(51)	$0.172(100) \times 10^{-3}$

Table 3: Long distance correction to ϵ_K as we vary the intermediate scale μ_{RI} . The fourth column is the sum of the results in the previous two column and the last column is the corresponding contribution to ϵ_K .

4. Conclusion

In this exploratory calculation with unphysical charm and light quark mass, we find a long distance correction to ϵ_K of $0.170(100) \times 10^{-3}$ (using the result of $\mu_{RI} = 2.11$ GeV), which is about

8% of the total ϵ_K experimental value. This is the correction that should be added to the Standard Model result of ϵ_K that is usually presented. In our method, instead of integrating the charm quark at zero external momentum and treating the bi-local operator as a local operator, we use a momentum μ_{RI} that can be chosen far above the charm quark mass (of course, this scale is limited by the inverse lattice spacing $1/a$) in this perturbative calculation. Therefore we have much better control of the systematic error in perturbation theory, and are able to evaluate the low-energy, non-perturbative part in our lattice calculation. Our matching to perturbation theory calculation for $\Delta Y_{\overline{MS}}(\mu_{RI})$ is done at NLO. To do this in NNLO, we must perform a two loop calculation which is significantly more difficult than our current one-loop perturbative calculation. The correction from NLO to NNLO to the Standard Model estimation to ϵ_K is only a few percent, but it may change our conclusion because the size of our long distance correction to ϵ_K is also at the 10% level.

We must note that this is not a physical calculation, in that we have a heavier than physical light quark mass which corresponds to a pion mass of 329 MeV. We also have an unphysical charm quark mass of 968 MeV, because we cannot go to a larger charm quark mass in our Iwasaki lattice with $1/a = 1.78$ GeV and a domain wall fermion action. A physical calculation with physical quark masses on a finer lattice will provide more realistic information than the current one.

References

- [1] Y. Aoki et al. Continuum Limit Physics from 2+1 Flavor Domain Wall QCD. *Phys. Rev.*, D83:074508, 2011.
- [2] Jon A. Bailey, Yong-Chull Jang, Weonjong Lee, and Sungwoo Park. Current status of ϵ_K with lattice QCD inputs. 2015.
- [3] Gerhard Buchalla, Andrzej J. Buras, and Markus E. Lautenbacher. Weak decays beyond leading logarithms. *Rev. Mod. Phys.*, 68:1125–1244, Oct 1996.
- [4] Andrzej J. Buras, Diego Guadagnoli, and Gino Isidori. On ϵ_K Beyond Lowest Order in the Operator Product Expansion. *Phys. Lett.*, B688:309–313, 2010.
- [5] N. H. Christ, T. Izubuchi, C. T. Sachrajda, A. Soni, and J. Yu. Long distance contribution to the $K_L - K_S$ mass difference. *Phys. Rev. D*, 88:014508, Jul.
- [6] Norman H. Christ and Ziyuan Bai. Computing the long-distance contribution to ϵ_k . *PoS(LATTICE 2015)342*, 2015.
- [7] Norman H. Christ, Xu Feng, Antonin Portelli, and Christopher T. Sachrajda. Prospects for a lattice computation of rare kaon decay amplitudes II $K \rightarrow \pi \nu \bar{\nu}$ decays. *Phys. Rev.*, D93(11):114517, 2016.